A Comparative Drivability Analysis for Autonomous Robots in Underground Mines Using the Entropy and SRM Models

Omowunmi Falola
ISAT Laboratory,
Department of Computer Science,
University of Cape Town,
Cape Town, South Africa.
ofalola@cs.uct.ac.za

Isaac Osunmakinde
Semantic Computing Group,
School of Computing,
College of Science,
Engineering and Technology
University of South Africa,
Pretoria, South Africa.
osunmio@unisa.ac.za

Antoine Bagula
ISAT Laboratory,
Department of Computer Science,
University of Cape Town,
Cape Town, South Africa.
bagula@cs.uct.ac.za

ABSTRACT

The mining industry is constantly faced with the dual needs for safety and improved productivity. It is widely recognized that robots can play a significant role in pre-disaster (pre-emption) and post-disaster (recovery) mine rescue operations. This would inevitably enhance productivity and greatly reduce human exposure to dangerous underground mine environment. Nonetheless, the success of a robot in a mine depends greatly on its visual capability to correctly interpret its immediate environment for navigational purposes. This work serves to assist robots' drivability in an underground mine. A probabilistic approach based on the local entropy is employed. The entropy is measured within a fixed window on a stream of mine frames to compute features used in the segmentation process. We then compare results using the statistical region merging (SRM) approach and evaluate the performance to provide useful qualitative and quantitative conclusions. Different regions of the mine, such as the shaft, stope and gallery, are investigated and results show that a good drivable region can be detected in an underground mine environment.

Categories and Subject Descriptors

I.4 [**Image Processing and Computer Vision**]: Segmentation—*region growing, partitioning and pixel classification*; I.2.9 [**Robotics**]: Sensors, Autonomous vehicles; I.2.10 [**Vision and Scene Understanding(I.4.8,I.5)**]: Intensity, color, photometry and thresholding

General Terms

Algorithms, Experimentation, Performance, Reliability.

Keywords

SRM, Entropy, Drivability, Region Detection, Navigation, Mine, Underground Terrains, and Robot

SAICSIT'12 October 01 - 03 2012, Pretoria, South Africa

1. INTRODUCTION

The mining industry of South Africa is a world class industry and a cornerstone of the South African economy. Figure 1 shows the growth in sales volume of South African mining products between the years 1987 and 2009 [41] and Figure 2 shows an overview of value distribution created by the mining industry [33]. In 2009, according to a report published by the Chamber of Mines of South Africa [4], the industry contributed:

- 8.8% directly, and 10% indirectly, to the country's GDP.
- Over 50% of merchandise exports.
- About 1 million jobs (500 000 directly).
- About 18% of gross investment (10% directly).
- Approximately 30% of capital inflows into the country's economy.
- 93% of the country's electricity-generating capacity.
- About 30% of the country's liquid fuel supply.
- Between 10% and 20% of direct corporate tax receipts (worth R10.5-billion).

While these benefits are derived from the mining industry, many risks are associated with the business of the extraction of an ore body. The needs for safety and efficiency in the mining industry have called for the serious attention of researchers and practitioners in recent time. The "Mine Health and Safety Act 1996" [17] stipulates that employers must ensure safety and maintain a healthy and safe mining environment for workers. In the history of mining, the mortality rate of miners has been alarming; numerous accidents and disasters have been recorded [25]. Over 256 miners were reported dead and more than 64,000 were injured in mining accidents in the decade between 1988 and 1998.

According to a report in 2011 [33], fatalities were still unacceptably high, in line with the trend experienced in the recent past. Figure 3 shows some accident rates of miners and their work experience. Much effort has been directed to mine safety in past decade as the consensus remains that one death is one too many. It is estimated that the safety performance of the South African mining industry must improve by at least 20% per year to reach,

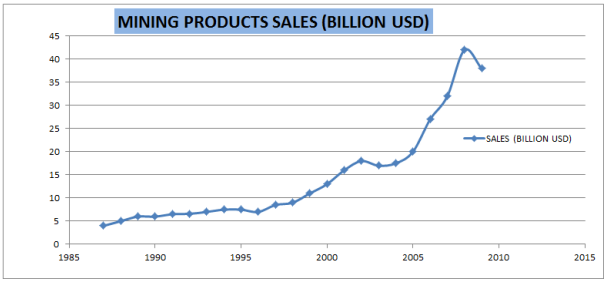

Figure 1: South African Sales Trend of Mining Products (B1 Information 2009, Department of Minerals and Energy)

the average performance of Australia, US and Canada [22] by 2013.

Underground mines' operation is associated with severe safety problems and the environments of mines tends to degrade fairly rapidly as mining progresses. Thus, the environment requires continuous investigation/monitoring for safe, effective and timely decisions of the management. Miners are susceptible to hazardous situations such as fall of ground, respiratory diseases associated with high level of dust, ergonomic hazards, falls in shafts, explosives, trucks and trams and unstable ground conditions. High fatality rates subject the mine industry to poor productivity. If a mine is unable to become more productive, it will go out of business, causing economic loss to the mining industry and the nation as a whole. Thus, creating a safe working environment for miners is not negotiable and would make mines remain as productive as possible in order to remain economically viable.

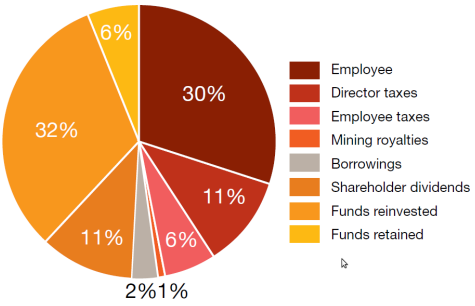

Figure 2: Distribution of Value Created by the Mining Sector

Safety is one of the key factors driving the trend to automation, which has attracted significant attention in recent years [10]. The significant potentials offered by autonomous robots have made them highly relevant in today's world [8]. To provide effective safety measures in mines, robots would play a crucial role. For example, robots can be sent to areas considered dangerous for human operation [37]. However for a robot to traverse a course effectively, its visual capability plays a key role. How the robot perceives and interprete its immediate environment is very important [13]. A significant part of artificial intelligence deals with planning or deliberation for system that can perform mechanical actions such as moving a robot through some environment. This type of processing (visual sensation) typically needs input data provided by a computer vision system, acting as a vision

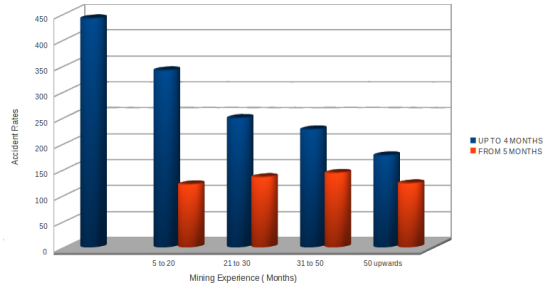

Figure 3: A Histogram Showing Total Mining Experience (in Months) and Accident Rates.

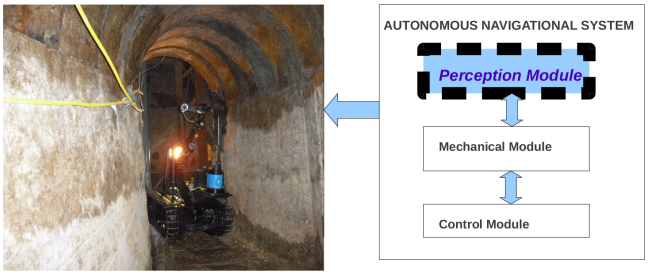

Figure 4: Overview of Autonomous Robot Navigation in the Mine

sensor and providing high-level information about the environment and the robot.

The human visual system (HVS) carries out recognition on image objects with ease. Activities such as sensing the environment, behavioral sequences and self propulsion are carried out by humans effortlessly. However, designing computer vision algorithms to imitate this is a challenging task [27]. Road following and autonomous path navigation requires an ability to discriminate between the road and surrounding areas and is a well-studied visual task [13, 27, 31]. However, its application to underground mining has generally not been explored in depth. Thus, it remains an ongoing key challenge

While robots have a great deal of potential to deal with safety issues in mines, an effective vision model is critical to their success. However, addressing robots' vision in underground terrains has received little attention in research. Drivable region detection for robots in a mine is a sound basis for navigation or path planning. Figure 4 depicts our idea of the autonomous robot's navigation in a mine. This research focuses on the perception module, a critical component in autonomous navigation, while the mechanical and control modules fall beyond the scope of this study. The perception module aims to capture observation of the environment (standard and high resolution imagery) based on the robots current position, and to specify which region is safe for robot's navigation. The major contributions of this paper are twofold:

- Firstly, application of the entropy and statistical region merging (SRM) models to drivability analysis of underground mines.
- Secondly, presentation of a visual assessment and quantitative evaluation of both models as a measure of their performance using publicly available mine images with a stream of images captured locally in an underground mine. [1, 2, 3].

To the best of our knowledge, despite being widely used to detect drivable regions for surface navigation, the entropy and SRM models have never been applied to an underground environment.

The rest of the paper is organised as follows: Section 2 presents a brief review of relevant literature. Section 3 presents the methodology and framework in detail. Section 4 follows with the experimental results and a review of the outcome measures for quatitative performance evaluation. Section 5 concludes the paper and future work are also presented.

2. THEORETICAL BACKGROUND

This section describes some work in the field of autonomous processes and image processing. The mathematical background to the entropy and SRM models is also documented in order to demonstrate the underlying principles of these models as employed in current research.

2.1 Related Work

The advancement in robotics and automation has led to a significant increase in autonomous processes. This has prompted the research community to develop new methods for autonomous navigation and even improve on existing ones [28] [31] [35]. Autonomous navigation in an underground mine environment has been studied for more than twelve years [34], a robust algorithm that is applicable in different terrains is yet to emerge. Thus, it remains an ongoing key challenge. Over the years, there has been some development in the field of image processing and segmentation, region classification and object detection for autonomous processes [7].

Greve *et al.* [19] report a new approach for the classification of image regions. They used wavelet standard deviation descriptor for texture patterns. The idea is to find a label for each region in any given image that can later be used in image management applications or retrieval systems e.g. to automatically tag inserted photos. The ultimate aim is to reduce the problem of image region classification to a problem of texture pattern classification.

Neuhaus *et al.* [29] investigate terrain drivability analysis in the 3D laser range data for autonomous robot navigation in unstructured environments. They used grid-based PCA and hierarchical PCA algorithms for classifying regions as either drivable or not and conducted a further examination using a novel algorithm, which determines the local terrain roughness.

Valarmathi and Aruna [40] proposed a novel approach to extract image features such as contour extraction and edge detection for image segmentation with self organizing properties for a network of adaptive elements. They used a type of neural network called Kohonen's self organising maps. The extra spatial information about a pixel region by using the unsupervised training algorithm verifies that the neighbouring pixels should have similar segmentation assignment unless they are on the boundary of two distinct regions.

From the literature, it is observed that most of the early studies on autonomous drivability analysis focus on outdoor navigation and ground-based detection. Underground terrains have received less attention, probably because of their roughness, compared to structured and unstructured ground-based terrains.

The state-of-the-art technology in mine automation includes a discussion on the various research projects and activities that have been carried out on the subject of automation of excavating machinery [21]. They stressed that the main tasks involved in autonomous loading are excavation, navigation, obstacle detection and avoidance. Nonetheless, most practical operations by robot in a mine have only been teleoperated [20] by a human and drivable region detection for robots in a mine has been scarcely addressed.

There has been a drift in robotics technology over the years with variations in application and phases of automation. The first-generation applications involve modification of conventional devices such as Load-Haul Dump (LHD) vehicles. The second phase of automation involves the creation of dedicated teleoperated robots while the third generation paradigm shift deals with autonomous robots in an exclusively robotic environment. Robotic technology has been extended to automated navigation of a LHD unit of underground mines. A roof mounted reflected line and a camera were used to guide the vehicle along the mine passages.

Bakambu *et al.* [9] describe an autonomous platform for navigation and surveying within networks of tunnels, as those typically found in underground mines and caves. The system works in two alternative modes: surveying mode or navigation mode. In the surveying mode, they gathered range data for map building using a remotely located supervisor who instructs the platform to move through successive sections of the network. In navigation mode, the supervisor specifies high-level missions using the previously acquired survey maps. A motion planner then translates each mission into a set of consecutive navigation actions separated by natural landmarks. Mission execution consists of autonomously detecting landmarks, self-localizing, and performing the planned navigation actions. The path following controller uses kinematical model of the motion vehicle, that depends on position (x, y) and orientation θ, while the wall following was ensured by following the middle axis of the drift.

Another initiative is the work of Clark *et al.* [16] that presented the development of an underwater robot system capable of mapping out and navigating underwater tunnel systems. They used the Simultaneous Localisation and Mapping (SLAM) techniques on a small underwater robot. A variation is presented by Aminossadati *et al.* [5], where computational fluid dynamics (CFD) modeling is used to simulate the airflow behavior in underground crosscut regions, where brattice sails are used to direct the airflow into these regions. This would help the mine ventilation designers meet the mine safety requirements.

With improved mine safety and productivity in mind [18], an innovative alternative to manual procedures is described for the application of carbon fiber and resin injection in concrete surfaces in tunnels. Vision and laser telemeter sensing are integrated into the tool to assure precise inspection and maintenance operations.

Lavigne *et al.* [24] investigated mapping GPS-deprived underground mining environments with the eventual goal of using these maps for navigation. The major goal of the work was to overcome the requirement for human input and to make the map building process autonomous. A similar problem is addressed by Hlophe [23]. Andreasson *et al.* [6] focus on methods to derive a high-resolution depth image from a low-resolution 3D range sensor and a colour image, they use colour similarity as an indication of depth similarity, based on the observation that depth discontinuities in the scene often correspond to colour or brightness changes in the camera image. This work hinges

on the work of Ferguson *et al.* [38], which deals with acquiring accurate and very dense 3D models in excavation sites and mapping of underground mines.

Our work focuses on the enhancement of robots' visual capability in underground mines by exploring drivability analysis of different regions in mines. This study uses two methods, which are the entropy and SRM models. These methods are used to extract features (colour and texture), thereafter image region segmentation and classification is carried out. The goal is to accelerate autonomous mine safety inspection tasks and consequently improve mine productivity.

2.2 Entropy Model

Entropy is defined as the number of binary symbols needed to code a given input given the probability of that input appearing on a stream. Entropy of an image is a statistical measure of randomness that can be used to characterize the texture of the input image [11]. High entropy indicates a high variance in the pixel values while low entropy is associated with fairly uniform pixel values. Since entropy is a measure of randomness, it provides a way to compare different regions (drivable and non-drivable regions) of the mine frames. The entropy of the mine images is computed using Equation (1) such that every pixel in the entropy filtered image (EFI) is measured within a fixed window (9×9 window in our case), which accounts for a reasonable percentage of the textural distribution of each pixel region.

The entropy for the pixel neighbourhood window is computed as shown in Equation (1).

$$k_i = \sum_v -q_v \times \log_2(q_v). \tag{1}$$

where q_i represents the probability that a random pixel p chosen from the window centered at p_v will have intensity i. The computation is done using the non-zero values of the histogram samples probability, say q_v, for every point, h, in the sample histogram as shown in Equation (2).

$$\textit{samples-probability}\ (q_v) = \frac{h}{\textit{length of histogram}}. \tag{2}$$

The entropy filter measures the relative change of entropy in a defined or sequential order [14]. For each pixel $p(i,j)$ in the EFI, there exists corresponding pixels $p_1, p_2, ..., p_N$ for each mine image. The local entropy k_i measured within a fixed window, for each pixel p_i in each image, is computed and the weighted average p is computed as shown in Equation (3).

$$p = \frac{\sum_{i=1}^{N} p_i k_i}{\sum_{i=1}^{N} k_i}. \tag{3}$$

2.3 Statistical Region Merging (SRM)

A region is a group of connected pixels with some homogeneity in feature property. Image segmentation refers to the process of partitioning a digital image into multiple regions (sets of pixels). Segmentation is a collection of methods allowing to interpret parts of the image as objects by transforming the pixels into visually meaningful partition of regions and object. The object is everything that is of interest in the image and the rest of the image is considered as the background. For an image I and homogeneity predicate H_p, the segmentation of an observed image I is a partition K of I into a set of G regions, $R_1, R_2, \ldots R_G$, such that the following conditions hold [12]:

a. $H_p(R_g) = true\ \forall g$

b. $H_p(R_g \cup R_h) = false\ \forall\ adjacent(R_g, R_h)$

c. $\bigcup_{g=1}^{G} R_g = I\ with\ g \neq h\ and\ R_g \cap R_h = \emptyset$

Statistical region merging (SRM) models segmentation as an inference problem by performing a statistical test based on a merging predicate and has been widely used in medical imaging and remote sensing imagery [14, 15, 30, 26]. In region merging, regions are iteratively grown by combining smaller regions or pixels. SRM uses a union-find data structure or merge-find set that is defined as follows:

- Find: Determines if two elements (pixels) are in the same subset.
- Union: Merges two subsets (sub-region) into a single subset (region) based on some criteria.

A major limitation of SRM is overmerging, where an observed region may contain more than one true region. It has been shown that the overmerging error is more or less insignificant as the algorithm manages an accuracy in segmentation close to optimum [30]. The idea is to reconstruct the statistical (true-similar) regions of an observed image instance.

The algorithm relies on the interaction between a merging predicate and the estimated cluster, Q, specified. The merging predicate, $P(R, R')$, on two candidate regions, R, R', is depicted in Equation (4) with an extension in Equations (5) and (6).

$$P(R,R') = \begin{cases} \text{true} & \textit{if} \quad \forall c \in (\text{R,G,B}), |\bar{R}'_c - \bar{R}_c| \leq T \\ \text{false} & \text{otherwise} \end{cases} \tag{4}$$

$$T = \left| \sqrt{k^2(R) + k^2(R')} \right|. \tag{5}$$

$$k(R) = g \sqrt{\frac{1}{2Q\,|R|} \ln(6|I|^2 R_{|R|})}. \tag{6}$$

R_c is the observed average colour channel c in region R and $R_{|R|}$ represents the set of regions with R pixels.

Let I be an observed image with pixels $|I|$ that each contains three (R, G, B) values belonging to the set $\{0, 1, \cdots, g-1$ pixels$\}$ where $g = 256$. The observed image I' is generated by sampling each statistical pixel for the three RGB channels. Every colour level of each pixel of I' takes on value in the set of Q independent random variables with values of $[0, g/Q]$. Q is a parameter that describes the statistical complexity of I', the difficulty of the problem and the generality of the model [26]. The optimal statistical regions in I' satisfy the property of homogeneity and separability.

- Homogeneity property: In any statistical region and given any colour channel, the statistical pixels have the same expectation value.
- Separability property: The expectation of any adjacent statistical region differ in at least one colour channel

Equation (7) defines the sort function [30], where p'_a, p_a represent pixel values of a pair of adjacent pixels of the colour channel.

$$f(p,p') = \max_{a \in R,G,B} |p_a - p'_a|. \tag{7}$$

3. PROPOSED SYSTEM MODEL FOR DRIVABILITY ANALYSIS

This section presents our methodology and give detailed description of the entropy and SRM approach to drivability analysis.

3.1 Proposed System Model

Our system approach is presented in this section. The entropy and SRM methods as discussed in the previous section are presented here. We also give useful qualitative and quantitative evaluation measures for performance checking. Figure 5 shows the overview of the system model.

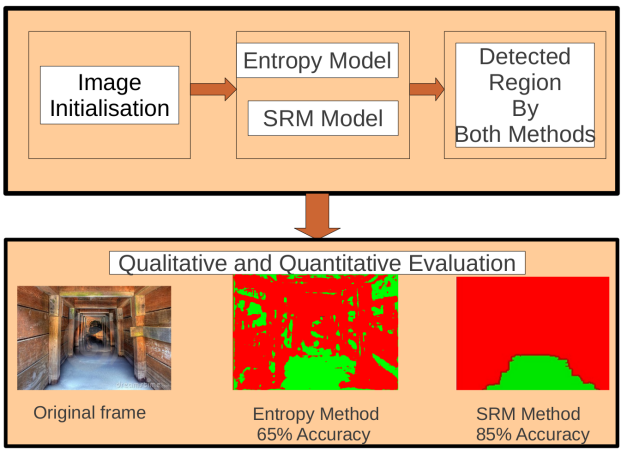

Figure 5: Overview of System Model

3.2 Entropy Approach to Drivability

Figure 8 describes the interlinked streams of the entropy approach used in this work.

3.2.1 Image Initialisation and Preprocessing

Image downsampling has become a regular operation during image processing for computational efficiency. However, conventional image downsampling methods do not accurately represent the appearance of the original image, and the perceived appearance of an image is altered when the resolution is lowered [39]. An image downsampling filter that preserves the appearance of blurriness in the lower resolution image is needed. Several downsampling options exists and the choice of downsampling varies for different applications but in this work, we use an appearance preserving downsampling filter called antialias. The choice of resolution for an image depends on the application at hand. The images used in this work were down-sampled to 300×225 resolution as part of the pre-processing stage.

Initial processing is usally carried out on raw data prior to data analysis. This is necessary to correct any distortion due to the characteristics of the imaging conditions and imaging system. The grayscale image used as the input is obtained by averaging the three RGB (reg, green, blue) colour channels for each pixel p in image I. In order to aid visual interpretation, the image contrast is enhanced with a histogram equalization as shown in Figure 6 and features were computed at each pixel location, P_i. Figure 6 shows the graphical representation of the number of pixels in an image as a function of their intensity. The x-axis shows the pixel intensity levels while the y-axis represents the number of pixels corresponding to each intensity level.

Let I be a given image represented as a P_r by q_r matrix of integer pixel intensities ranging from 0 to $L-1$, where L is the number of possible intensity values, often $L = 256$. Let k denote the normalized histogram of I. Then

$$k_n = \frac{\text{number of pixels with intensity } n}{\text{total number of pixels}} \quad n = 0, 1, ..., L-1. \tag{8}$$

The histogram equalized image, say $k^{'}$, will be defined as

$$k^{'}_{i,j} = \text{floor}((L-1)\sum_{n=0}^{f_{i,j}} k_n). \tag{9}$$

The floor of x depicted $\lfloor x \rfloor$ is defined as the nearest integer $\leq x$. Equation (9) is equivalent to transforming the pixel intensities, p, of I by the function

$$T(p) = \text{floor}((L-1)\sum_{n=0}^{p} k_n). \tag{10}$$

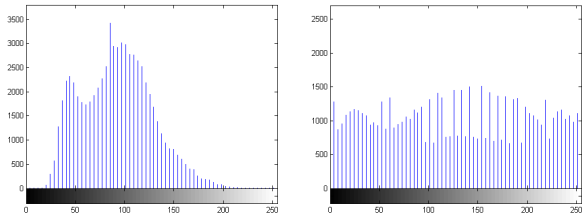

Figure 6: Image Histogram and the Corresponding Transformed Histogram

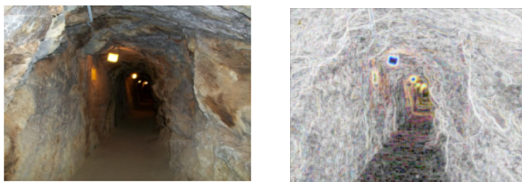

Figure 7: Original Frame and the Corresponding Entropy Filtered Image

3.2.2 Image Segmentation

In this research, the purpose of segmentation is to identify the navigation area in the mine images, that is, the image, I, into two types of objects: drivable and non-drivable areas. Figure 7 shows a mine frame and the corresponding entropy filtered image obtained according to the description in Section 2.2. One way to apply the entropy concept to image segmentation is to calculate the graylevel transition probability distributions of the co-occurrence matrices for an image and a thresholded bilevel image, respectively, then find a threshold which minimizes the discrepancy between these two transition probability distributions, i.e. their relative entropy. The threshold rendering the smallest relative entropy will be selected to segment the image.

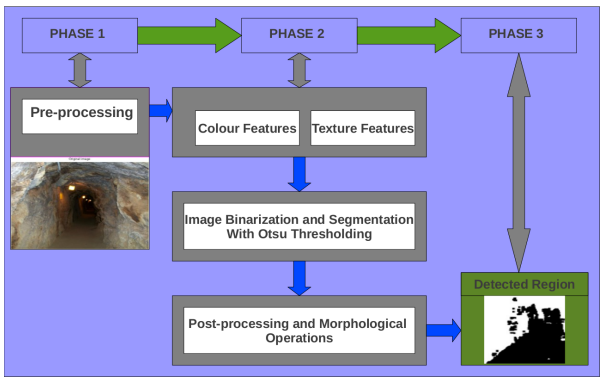

Figure 8: Block Diagram of Entropy Model

In this work, after pre-processing the image and computing the texture features, we begin the search for an ideal threshold using a segmentation technique proposed by Otsu [32]. The Otsu method finds the threshold that minimizes the weighted within-class variance of the image and invariably maximizes the between-class variance of the image. Otsu calculates the optimum threshold separating those two classes so that their combined spread (intra-class variance) is minimal, maximizing the separation between object and background. The process of finding the optimal threshold is iterative, starting from an arbitrary value. The iterative threshold is set to stop when the change in threshold value is insignificant. This indicates that the threshold is very close to optimum. The mean values are computed by summing the product of each intensity and the corresponding histogram proportion. The sum is then divided by the total sum of the pixel intensity values to get the average.

In general, the thresholding process is seen as the partitioning of pixels of an image in two classes: P_1 (object) and P_2 (background). This method is recursive and searches the maximization for the cases: P_1 (0,1,..., T) and P_2 ($T+1, T+2, ..., L-1$), where T is the chosen optimal threshold and L the number of intensity levels of the image. Otsu thresholding method exhaustively search for the threshold that minimizes the intra-class variance $\sigma^2_\omega(t)$ defined in Equation (11) as a weighted sum of variances of the two classes.

$$\sigma^2_\omega(t) = \omega_1(t)\sigma^2_1(t) + \omega_2(t)\sigma^2_2(t). \quad (11)$$

Otsu Thresholding

Step 1: Estimate histogram and probabilities of each intensity level
Step 2: Set up initial $\omega_i(0)$ and $\mu_i(0)$
Step 3: Search all possible thresholds $t = 1 \ldots L$;

1. Update class probability (ω_i) and class mean(μ_i).
2. Compute $\sigma^2_b(t)$.

Step 4: The optimal threshold T corresponds to max $(\sigma^2_b(t))$

3.2.3 *Morphological Operations*

Morphological operations are often used to understand the structure of an image. In this work, the main morphological operation utilised can be likened to flood-filling, which are referred to as erosion and dilation. The two operations are explained below:

- Dilation: In dilation, the output value of an image pixel is the maximum value of all the pixels in the input pixel's neighborhood. Thus, dilation broadens the boundaries of regions of white pixels. This is usually done with the support of a structuring element S_e with specified neighbourhood, which in our case is a 9×9 neighbourhood. The 9×9 neighbourhood is used to perform a sliding window operation on the image for the step-wise decision making processes.

- Erosion: This is also known as morphological closing. The decision making process also uses the 9×9 neighbourhood where the pixel value of the output pixel is the minimum value of all the pixels in the input pixel's neighborhood.

The initial assumption is that the entropy would return similar probabilistic distribution for pixel regions sharing the same textural properties (i.e. drivable area) within a mine frame. However, this cannot be guaranteed in its entirety as there could be some interference (noisy pixels) in the processed mine frame. Morphological operations help in reducing such interference by removing isolated blocks within a mine image and thereafter revealing large area of connected pixels. The erode/dilate filter helps to remove small wrong areas (areas with some noise). Figure 9 shows an example of the effect of morphological operation on a mine frame.

Figure 9: Morphological Operation on Image Classification

3.3 SRM Approach to Drivability Analysis

The SRM algorithm has two important criteria: the merging predicate and specified cluster Q, which determines the number of segments/regions, for the input image. SRM is noted for its computational efficiency, simplicity and good performance as seen in section 4.3. The flexibility of Q is a major advantage as a trade-off parameter that is adjusted to obtain a compromise between the observed results and the strength of the model. In our experiment, after testing with different values of Q, the value $Q = 32$ gave the optimal result for the image classification. Q is a parameter that controls the coarseness and busyness of the classification. Figure 10 presents the flow of the algorithm.

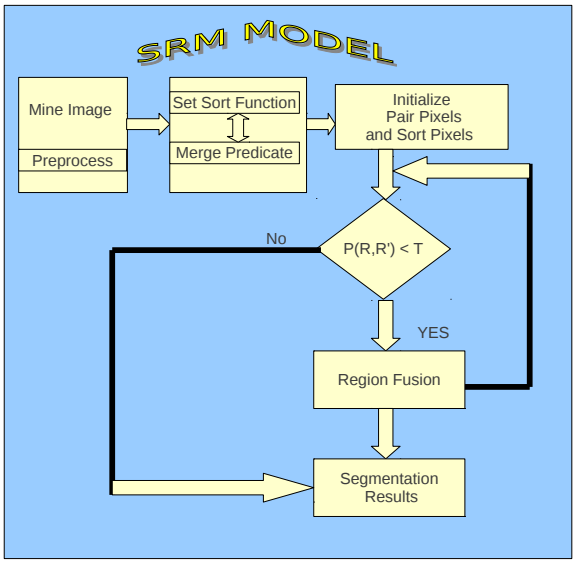

Figure 10: Flow of SRM Model

The algorithm uses a 4-connectivity scheme to determine adjacent pixels relative to the center pixel (in green) as shown in Figure 11. The pixels are sorted in ascending order based on the sort function in Equation (7). Thereafter, the algorithm considers every pair of pixels (p, p') of the set D_I and performs the statistical test based on the merging predicate. If the regions of the pixels differ and the mean intensity are sufficiently similar enough to be merged, then the two regions are merged.

The SRM method presents the list of pixels belonging to each segmented region with their average mean intensities. We focus on the pixels region which forms clusters at the base of each observed image I towards the midpoint when scanning from the left. This forms the pixel region closer to the robots view and thus, the drivable part as can be seen in the test cases presented.

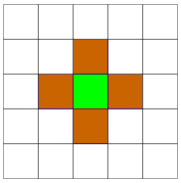

Figure 11: Depiction of the Four-Connectivity Scheme

Pseudocode for SRM Algorithm

Step 1: Initialise image I and estimated segments Q
Step 2: D_I = {the 4-connectivity adjacent pixels}
Step 3: $\bar{D_I} = sort(D_I, f)$
While $\bar{D_I} \neq \emptyset$
for i = 1 to $|\bar{D_I}|$ do
Step 4: if $(((P(R_{(p_i')}, R_{(p_i)}) == true)\ and\ (R_{(p_i')} \neq R_{(p_i)}))$
then merge regions $(R_{(p_i')}, R_{(p_i)})$

3.4 Evaluation Mechanism

We give a qualitative and quantitative (confusion matrix) evaluation approach as a measure of performance of the two methods described in this work. The qualitative evaluation which is the visual comparison is presented in Sections 4.1, 4.2 and 4.3. The quantitative evaluation is presented in Section 4.4. In this work, we considered the confusion matrix validation technique. We repeated the confusion matrix procedure n times, with $n \in \{3, 5\}$, where each n subsamples are used exactly once as the validation data. The idea is to evaluate the accuracy level (hit rate) of the algorithms (entropy and SRM) in the following context.

- True positives (TP): The number of drivable pixels correctly detected (correct matches).
- True Negatives (TN): The non-matches pixels that were correctly rejected.
- False Positives (FP): The proposed pixel matches that are incorrect.
- False Negatives (FN): The proposed pixel matches that were not correctly detected.

Thus, the accuracy (acc %) is given as;

$$\text{Acc} = \frac{\text{TP} + \text{TN}}{\text{TP} + \text{TN} + \text{FP} + \text{FN}} \times 100\% \qquad (12)$$

4. EXPERIMENTAL EVALUATION

The major focus in this work is feature extraction and classification for front view mine frame detection in order to enhance the visual capability of autonomous robots in underground mines. For the images experimented in this work, different test cases of mine frames were carefully chosen from publicly available mine images and some were captured from a local mine using the common photo cameras [1, 2, 3]. The test cases are a representative of different regions, such as shaft, stope and gallery, in an underground mine environment. We chose the images to represent a wide variety of terrains and contexts. Some of the images contain a single complete object (occlusion) in the portion of the images and some have no objects. We tested the entropy and SRM method on a stream of rough mine frames and performance evaluation is carried out to provide useful qualitative and quantitative conclusions.

4.1 Experiment 1: Observation on the Entropy Approach

In this section we present some results obtained on a stream of mine frames using the entropy approach. Figure 12 shows the visual assessment of the entropy method on some mine frames. The first row of Figure 12 consists of original mine frames, the second row presents the entropy filtered images while the third row is the result of Otsu thresholding. The last row presents the final detection with the RGB (red, green, blue) representation of the corresponding mine frames, the lower (green) regions forms the drivable part while the upper (red) regions forms the non-drivable part. We observe that the results produced by the entropy approach tend to be affected by the effect of strong shadow regions on the tested frames. This can be seen in the qualitative results, as most of the connected regions produced in some of the frames are in the shadow areas.

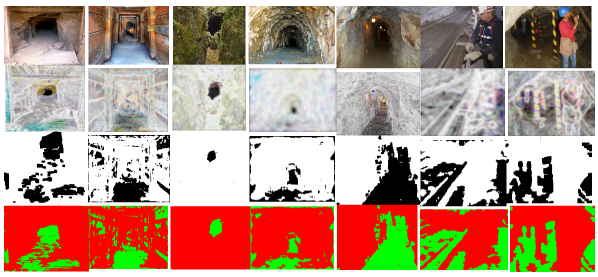

Figure 12: Qualitative Results of Entropy Approach on Some Mine Frames

Figure 13: Qualitative Results of SRM Method on Some Mine Frames

4.2 Experiment 2: Observation on the SRM Approach

In this section, we present some of the results obtained using the SRM method as shown in Figure 13. The first row are the original mine frames. The second row presents the results of the clusters generated for regions with homogeneity. The third row gives the RGB representation of the drivable regions extracted for corresponding frames. The base (green colour) regions indicates the drivable region while the upper (red colour) regions represents the non-drivable region. It is evident from these results that SRM has the ability to reconstruct the structural components and retain clusters of the mine images that are closer to the robot's view. Pixels closer to the robot's view tend to form most of the drivable region.

4.3 Qualitative Comparison of Entropy and SRM on Mine Frames

The visual comparison of the entropy and SRM methods is presented in Figure 14. In the experiment, the images in the first row are the original mine images, the images in the second row are results of drivable regions detected using the entropy approach while the third row presents the drivable regions detected for corresponding frames using the SRM approach. The lower (green colour) regions indicate the drivable regions while the upper (red) represent the non-drivable regions. It can be seen from the results that the two regions (drivable and non-drivable) were clearly distinguished in almost all the tested scenarios using the SRM approach.

4.4 Quantitative Comparison of Entropy and SRM on Mine Frames

We conducted experiments to evaluate the quantitative performance of both entropy and SRM approaches to drivability. We utilised the confusion matrix validation process n times ($n \in \{3, 5\}$). Pixel points are selected randomly from the image data I_d with the aid of an automated code (10 pixels per time for n-fold validation, making 30 pixels per frame [30 frames = 900 pixels] for 3-fold and 50 pixels per frame [30 frames = 1500 pixels] for 5-fold). The correctness of the pixel (i, j) is evaluated based on its current classification position(x, y) in the detected frame relative to its position (x, y) in the original frame. The estimated confusion matrix validation accuracy is the overall number of correct classification divided by number of instance in the image-data I_d [36]. Table 1 shows the quantitative performance of the algorithms with $n = 3$ and $n = 5$.

5. CONCLUDING REMARKS

Computer vision is a challenging area and much research is still being carried out in this area with little attention to underground terrains. In this work, we aim to achieve autonomous drivable region detection in underground mine environments. This work has demonstrated the feasibility of enhancing robots' capability in identifying drivable regions within a mine environment. Different regions of mines representing a wide variety of terrains ranging from the stope, shaft and gallery are investigated.

The entropy approach and the SRM algorithm are adopted as means of identifying drivable regions within a mine frame. The performance of both entropy and SRM methods in drivability analysis are evaluated. Results show that SRM outperforms the entropy approach in almost all the scenarios and detection of an underground terrain can be achieved. Using the entropy approach, the computed local entropy gives useful textural information about the pixel distribution. The entropy returns probabilities of the randomness of the pixel, p_i, gray tone within a fixed window. The probabilistic textural information was used in the mine image classification together with Otsu thresholding. The SRM algorithm, on the other hand, is able to reconstruct the main structural components of the underground mine imagery by a simple but effective statistiscal analysis. The SRM method worked well on a variety of mine frames tested as shown in Figures 13 and 14 and Table 1. It can be seen from the results that the two regions (drivable and non-drivable) were clearly distinguished mostly with the SRM method.

The major focus in this work is feature extraction and classification for front view mine frame detection. This would in-turn enhance autonomous robots visual capability to identify drivable region within the mine environment. The result of this work is a useful application that would accelerate further motion and path planning (control and mechanical decisions) for autonomous robots' navigation within underground terrains. The solution presented in this work would enhance the development of a platform for performing autonomous safety inspections and any other autonomous task within underground mine environments.

We aim to improve on the current classification results and utilise more machine learning algorithms in mine frame detection for better performance and future adoption. Furthermore, alternate methods of performing drivability analysis can be explored using some sort of distance sensors. The laser or XBOX kinect 3D sensors in acquiring depth maps would result in useful 3D drivability analysis. In addition, drivability analysis can be explored to handle environmental noise, such as shadow.

6. ACKNOWLEDGMENTS

The authors gratefully acknowledge resources made available by UCT and UNISA, South Africa.

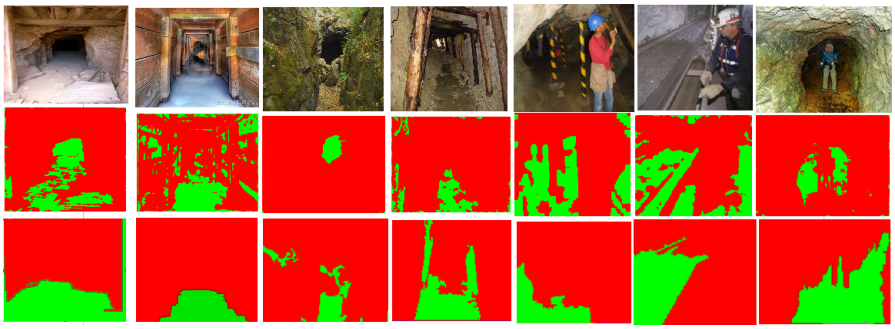

Figure 14: Visual Comparison of Entropy and SRM on Some Mine Frames

Table 1: Comparing Drivability Analysis of Underground Terrains Using the Entropy and SRM Algorithms

Terrain	Algorithms	n-fold confusion matrix validation	Correctly classified pixels (TP, TN)	Incorrectly classified pixels (FP, FN)	Accuracy of detection (%)
Underground mines (30 image frames)	Entropy	3	520	380	57.78
		5	815	685	54.33
	SRM	3	745	155	82.78
		5	1200	300	80.00

7. REFERENCES

[1] Istock photo, June 2009. Available from: http://www.istockphoto.com/stock-photo-2164196-old-mine.php

[2] Spelunking safety, May 2009. Available from: http://brettberk.com/2009/05/

[3] Gold mining and historical documentation, May 2012. Available from: http://www.ironminers.com/

[4] Mining and minerals in south africa, March 2012. Available from:http://www.southafrica.info/business/economy/sectors/

[5] S. M. Aminossadati and K. Hooman. Numerical simulation of ventilation air flow in underground mine workings. In *12th U.S./North American Mine Ventilation Symposium*, pages 253–259. University of Queensland, June 2008.

[6] H. Andreasson, R. Triebel, and A. Lilienthal. Vision-based interpolation of 3D laser scans. In *Proceedings of IEEE International Conference on Autonomous Robots and Agents*, pages 469–474. ICARA, August 2006.

[7] A. Angelova, L. Matthies, D. Helmick, and P. Perona. Fast terrain classification using variable-length representation for autonomous navigation. In *Proceedings of IEEE Conference on Computer Vision and Pattern Recognition*, pages 1–8. CVPR, March 2007.

[8] A. Angelova, L. Matthies, D. Helmick, and P. Perona. Learning slip behaviour using automatic mechanical supervision. In *Proceedings of IEEE International Conference on Robotics and Automation*, pages 1741–1748. ICRA group, April 2007.

[9] J. N. Bakambu and V. Polotski. Autonomous system for navigation and surveying in underground mines. *Journal of Field Robotics*, 24(10):829–847, October 2007.

[10] L. K. Bandyopadhyay, S. K. Chaulya, P. K. Mishra, and A. Choure. Wireless information and safety system for underground mines. In *Proceedings of the International Union of Radio Science*, pages 1–4. URSI Chicago, August 2008.

[11] S. Battiato. Entropy and gibbs distribution in image processing: An historical perspective. *University of Catania*, 6(1):1–21, November 2001.

[12] S. Battiato, G. Farinella, and G. Puglisi. SVG vectorization by statistical region merging. In *Proceedings of the 4th Conference Eurographics Italian Chapter*, pages 15–21. The Eurographics Association, February 2006.

[13] J. Benjamin, Y. Papelis, R. Pillat, G. Stein, and D. Harper. A practical approach to robotic design for the DARPA urban challenge. *Journal of Field Robotics*, 25(8):528–566, July 2008.

[14] F. Calderero and F. Marques. Region merging techniques using information theory statistical measures. *IEEE Transactions on Image Processing*, 19(16):1567–1586, June 2010.

[15] M. E. Celebi, H. A. Kingravi, J. Lee, W. Stoecker, J. M. Malters, H. Iyatomi, Y. A. Aslandogan, R. Moss, and A. A. Marghoob. Fast and accurate border detection in dermoscopy images using statistical region merging. *James Schlipmann Melanoma Cancer Foundation and NIH (SBIR 2R44 CA-101639-02A2)*, 1(16):1–10, July 2006.

[16] C. Clark, C. Olstad, K. Buhagiar, and T. Gambin. Archaeology via underwater robots: Mapping and localization within maltese cistern systems. In *Proceedings of the 10th IEEE International Conference on Control, Automation, Robotics and*

Vision, pages 662–667. ICARCV, December 2008.

[17] J. S. Editor. Juta's statutes of south africa. *Twentieth Edition ISBN 978 0 7021 8472 7*, 6:2–89, November 2010.

[18] J. C. Gonzàlez, S. Martìnez, A. Jardòn, and C. Balaguer. Robot-aided tunnel inspection and maintenance system. In *Proceedings of the 26th International Symposium on Automation and Robotics in Construction*, pages 420–426. Austin TX, U.S.A., August 2009.

[19] S. Greve, M. Grzegorzek, C. Saathoff, and D. Paulus. Classification of image regions using the wavelet standard deviation descriptor. In *Proceedings of the International Multiconference on Computer Science and Information Technology*, pages 703–708. IMCSIT, October 2010.

[20] D. W. Hainsworth. Teleoperation user interfaces for mining robotics. *CSIRO Exploration and Mining, Brisbane, Qld 4069 Australia*, 11(1):19–28, July 2001.

[21] A. Hemami and F. Hassani. An overview of autonomous loading of bulk material. In *26th International Symposium on Automation and Robotics in Construction*, pages 405–411. ISARC, November 2009.

[22] M. A. Hermanus. Occupational health and safety in mining- status, new developments and concerns. *Journal of the Southern African Institute of Mining and Metallurgy*, 107(1):531–538, May 2007.

[23] K. Hlophe. Gps-deprived localisation for underground mines. In *Proceedings of CSIR 3rd Beinnual Conference on Science Real and Relevant*, page 1. Pretoria, South Africa, August 2010.

[24] N. J. Lavigne, J. A. Marshall, , and U. Artan. Towards underground mine drift mapping with RFID. In *Proceedings of the 23rd IEEE Canadian Conference on Electrical and Computer Engineering*, pages 1–6. University of Carleton, May 2010.

[25] J. P. Leger. Trends and causes of fatalities in South African mines. *Journal of Safety Science*, 14(3-4):169–185, May 1991.

[26] H. Li, H. Gu, Y. Han, and J. Yang. An efficient multiscale SRMMHR (statistical region merging and minimum heterogeneity rule) segmentation method for high resolution remote sensing imagery. *IEEE Journal of Selected Topics in Applied Earth Observations and Remote Sensing*, 2(2):67–73, June 2009.

[27] J. Minguez and L. Montano. Sensor-based robot motion generation in unknown, dynamic and troublesome scenarios. *Journal of Robotics and Autonomous Systems*, 52(4):290–311, July 2005.

[28] J. Minguez and L. Montano. Extending collision avoidance methods to consider the vehicle shape, the kinematics, and dynamics of a mobile robot. *IEEE Transactions on Robotics*, 25(2):367–381, April 2009.

[29] F. Neuhaus, D. Dillenberger, J. Pellenz, and D. Paulus. Terrain drivability analysis in 3D laser range data for autonomous robot navigation in unstructured environments. In *Proceedings of IEEE international conference on Emerging Technologies and Factory Automation*, pages 1–4. Active Vision Group, University of Koblenz-Landau, Germany, September 2009.

[30] R. Nock and F. Nielsen. Statistical region merging. *IEEE Transactions on Pattern Analysis and Machine Intelligence*, 26(11):1–7, November 2004.

[31] I. Osunmakinde and T. Ndhlovu. Ground plane detection for autonomous robots in complex environments inclined with flexed far-field terrains. In *Proceedings of the 14th IASTED International conference on robotics and applications*, pages 664–095. Cambridge, Massachusetts, USA, ACTA Press, November 2009.

[32] N. Otsu. A threshold selection method from gray-level histograms. *IEEE Transactions on Systems, Man and Cybernetics*, 9(1):62–66, January 1979.

[33] PricewaterhouseCoopers("PwC"). Review of trends in the South African mining industry. *South African Mine*, 6(1):1–48, November 2011.

[34] S. Scheding, G. Dissanayake, E. Nebot, and H. Durrant-Whyte. An experiment in autonomous navigation of an underground mining vehicle. *IEEE Transactions on Robotics and Automation*, 15(1):85–95, February 1999.

[35] N. Senthilkumaran and R. Rajesh. Edge detection techniques for image segmentation- a survey of soft computing approaches. *International Journal of Recent Trends in Engineering*, 1(2):250–254, May 2009.

[36] T. Fawcett. An introduction to ROC analysis. *Pattern Recognition Letters*, 27(1):861–874, December 2005.

[37] S. R. Teleka, J. J. Green, S. Brink, J. Sheer, and K. Hlophe. The automation of the 'making safe' process in South African hard-rock underground mines. *International Journal of Engineering and Advanced Technology*, 1(4):1–7, April 2012.

[38] S. Thrun, D. Hähnel, D. Ferguson, M. Montemerlo, R. Triebel, W. Burgard, C. Baker, Z. Omohundro, S. Thayer, and W. Whittaker. A system for volumetric robotic mapping of abandoned mines. In *Proceedings of IEEE International Conference on Robotics and Automation*, pages 4270–4275. ICRA Taiwan, September 2003.

[39] M. Trentacoste, R. Mantiuk, and W. Heidrich. Blur-aware image downsampling. *Journal of Eurographics*, 30(2):1–10, April 2011.

[40] P. Valarmathi and M. Aruna. A novel approach for image segmentation using SOM. *International Journal of Computer Science and Technology*, 2(1):84–85, December 2011.

[41] J. van der Merwe. Future of the South African mining industry and the roles of the SAIMM and the universities. *Journal of the Southern African Institute of Mining and Metallurgy*, 111(9):581–592, September 2011.